Journal of Catalysis 277 (2011) 27–35

Contents lists available at ScienceDirect

Journal of Catalysis

journal homepage: www.elsevier.com/locate/jcat

Deuterium kinetic isotopic study for hydrogenolysis of ethyl butyrate

Muthu Kumaran Gnanamani, Gary Jacobs, Robert A. Keogh, Burtron H. Davis *

Center for Applied Energy Research, University of Kentucky, 2540 Research Park Dr., Lexington, KY 40511, United States

ARTICLE INFO

Article history:
Received 23 June 2010
Revised 30 September 2010
Accepted 12 October 2010
Available online 12 November 2010

Keywords:
Hydrogenolysis
Deuterium isotope effect
Ethyl butyrate
n-Butyric acid
n-Butyraldehyde
DRIFTS

ABSTRACT

The hydrogenation of ethyl butyrate, *n*-butyric acid, and *n*-butyraldehyde to their corresponding alcohol(s) has been studied over a γ-Al_2O_3-supported cobalt catalyst using a high-pressure fixed-bed reactor in the temperature range of 473–493 K. H_2–D_2–H_2 switching experiments show that ethyl butyrate and *n*-butyric acid follow an inverse kinetic isotope effect (KIE) (i.e. r^H/r^D = 0.50–0.54), whereas *n*-butyraldehyde did not display any KIE (i.e. r^H/r^D = 0.98). DRIFTS experiments were performed over the support and catalyst to monitor the surface species formed during the adsorption of ethyl butyrate and *n*-butyric acid at atmospheric pressure and the desired temperature. Butanoate and butanoyl species are the stable surface intermediates formed during hydrogenation of ethyl butyrate. Hydrogenation of butanoate to a partially hydrogenated intermediate is likely involved in the rate-determining step of ethyl butyrate and butyric acid hydrogenation.

1. Introduction

Hydrogenation of esters to alcohols is a well-known large-scale industrial process [1]. Several processes, which include the hydrogenolysis of an ester, have been proposed for the manufacture of basic chemicals such as methanol and ethanol. Hydrogenation of esters may give products such as alcohols [1], acids, hydrocarbons [2–4], and ethers [5], depending on the reaction conditions, the structure of the substrate, and the choice of catalyst. Copper-containing catalysts are widely used for the conversion of methyl acetate to methanol. Over the past several years, new catalysts have been developed as potential replacements for the existing catalyst system, including the identification of several promising catalysts based on copper [6].

Similarly, numerous catalytic systems have been proposed for hydrogenolysis of carboxylic acids. Typically, Cu-chromite-based catalysts have been used for the vapor-phase hydrogenolysis of acids [7]. Later, Kitson and Williams [8] demonstrated that bimetallic Pd–Re catalysts were active for hydrogenolysis of a variety of aliphatic monocarboxylic acids.

Regarding ester hydrogenolysis, Yan et al. [9] studied the liquid-phase hydrogenolysis of butyl acetate over a barium-promoted copper chromite catalyst at 50–200 atm and temperatures between 175° and 250 °C and found that additives such as calcium hydride increased the reaction rate. Evans et al. [10] showed that copper on silica, or even pure Raney copper, can be effective for the hydrogenolysis of esters. Claus et al. [11] investigated the hydrogenolysis of methyl and ethyl acetate over supported Group VIII metals at temperatures ranging from 493 K to 553 K under pressures up to 4 MPa. Pd/Al_2O_3 displayed no detectable activity toward hydrogenolysis of ethyl acetate. In contrast, Co/TiO_2 was found to exhibit considerably higher activity and selectivity to ethanol for the hydrogenolysis of methyl acetate. Van de Scheur and Staal [12] found that addition of a small amount of Zn to silica-supported copper catalysts enhanced their activity and selectivity to alcohol during hydrogenolysis of methyl acetate. The authors attributed this effect to Zn, which played an important role in the activation of the reactants.

According to Sorum and Onsager [13], the mechanism for hydrogenation of methyl formate over commercial copper chromite catalyst involves the formation of hemiacetal intermediate, which is then hydrogenated to methanol. In another study, Agarwal et al. [14] indicated that hydrogenolysis of ethyl acetate proceeds via dissociative adsorption of the ester using Cu/SiO_2, followed by slow hydrogenation of the acetyl fragment. On the other hand, they found that formate hydrogenolysis proceeds through the reaction of undissociatively adsorbed formate [14]. In most of the studies of ester hydrogenolysis found in the open literature, inactive supports like SiO_2 were used; thus, the major chemistry must take place on metallic sites (e.g., activation of C–O of esters). In contrast, γ-Al_2O_3 and TiO_2 are known to chemisorb esters [15–17], resulting in the formation of stable surface intermediates like acetates, which eventually undergo hydrogenation to finally produce an alcohol. In this study, our objective was to investigate the deuterium KIE for hydrogenation of ethyl butyrate and its oxygenated analogs (e.g., *n*-butyric acid and *n*-butyraldehyde) on a γ-Al_2O_3-supported cobalt catalyst using a differential

* Corresponding author. Fax: +1 859 257 0302.
E-mail address: davis@caer.uky.edu (B.H. Davis).

0021-9517/$ - see front matter © 2010 Elsevier Inc. All rights reserved.
doi:10.1016/j.jcat.2010.10.006

high-pressure fixed-bed reactor. DRIFTS experiments were performed for the support and catalyst to examine the surface species generated during the adsorption of reactants at elevated temperatures. By comparing these results, a plausible mechanism was proposed for the hydrogenation of ethyl butyrate and butyric acid over 25% Co/γ-Al_2O_3.

2. Experimental

The catalyst used in this study was cobalt supported on γ-Al_2O_3, which was prepared from a commercially available γ-Al_2O_3 support (Catalox 150). Cobalt was introduced to the support by the slurry phase impregnation method, whereby the aqueous solution of cobalt nitrate was 2.5 times the pore volume of the support. Due to the solubility limit of cobalt nitrate, two sequential impregnation and drying steps were used, the latter carried out using a rotary evaporator under vacuum. After impregnation with 25 wt.% of cobalt, the catalyst was dried at 373 K and then calcined in flowing air at 623 K for 4 h.

Nitrogen physisorption over the catalyst sample was carried out at 77 K using a Micromeritics Tri-Star instrument. The sample was first outgassed overnight at 433 K to 50 mTorr. The specific surface area of the catalyst was estimated by the BET method to be 103 m^2/g, while the single point pore volume was 0.258 cm^3/g cat. and the average pore radius was 5.0 nm.

DRIFTS experiments were carried out using a Nicolet Nexus 870 equipped with a DTGS–TEC detector to monitor the various surface species produced during the adsorption of reactants following activation with H_2 at elevated temperatures. A high-pressure/high-temperature chamber fitted with ZnSe windows was utilized as the catalyst holder. The gas lines leading to and from the IR cell were heat traced, insulated with ceramic fiber tape, and further covered with general purpose insulating wrap. Ethyl butyrate (EB) and *n*-butyric acid (BA) were introduced to the IR cell using 5 μL injections with a gas-tight syringe, and the carrier gas used was helium. Scans were taken at a resolution of 4 to give a data spacing of 1.928 cm^{-1}. Typically, 512 scans were taken to improve the signal to noise ratio. The catalyst was initially activated with H_2 at 773 K for 12 h before adsorbing the probe molecule (EB or BA) at the desired temperature. Similar experiments were performed over γ-Al_2O_3 as well in order to see the differences in the adsorbing behavior of EB between the support (γ-Al_2O_3) and catalyst (25% Co/γ-Al_2O_3). H_2-TPD was carried out after adsorbing EB on γ-Al_2O_3 and 25% Co/γ-Al_2O_3 at 473 K to determine the stability of the intermediate species formed over the surface of the catalyst in the temperature range of 473–623 K.

Reactions were conducted using a microcatalytic reactor system capable of operating at high pressures and temperatures. Liquid feed at the desired space velocity was introduced using a Milton Roy mini-piston pump. Hydrogen gas flow rates were metered using mass flow controllers (Brooks Instruments Model 5810B). The reactor portion of this system consisted of a $1/2 \times 21$ inch plug-flow microreactor. The catalyst was held in place by a bed of quartz wool. Typical catalyst charges in this unit were approximately 1.5 g of unreduced 25% Co/γ-Al_2O_3 along with 3.0 g of SiC diluent. All chemicals (i.e., ethyl butyrate (EB), *n*-butyric acid (BA), and *n*-butyraldehyde) were of high purity (>99.5%) and purchased from Sigma Aldrich. The catalyst was activated for 15 h at 623 K using a H_2:He (1:3) mixture. Total conversion of reactants for each experiment was kept below 15–20% in order to keep the reaction under differential operating conditions except during the hydrogenation of *n*-butyraldehyde.

Conversion has been defined as number of moles of ester converted per mole of ester introduced. To account for the change in number of moles during reaction, selectivity was defined such that the total selectivity of all carbon-containing products equaled 100%. The product gas stream exiting the reactor system was passed through a trap at 273 K to separate liquid and gas products. Gas-phase products (C_1–C_4) were analyzed using a micro GC (HP Quad series, Refinery Gas Analyzer) equipped with a TCD detector, while the liquid products condensed in the 273 K trap were analyzed separately using a HP 5890 GC with DB-5 capillary column. The deuterium switch was made after reaching steady-state conversion of reactants (EB, BA, and butyraldehyde) in order to measure the deuterium KIE for hydrogenation of ethyl butyrate, butyric acid, and butyraldehyde, respectively. The products containing deuterium (especially 1-butanol and ethyl alcohol) were analyzed by GC–MS.

3. Results and discussion

3.1. Hydrogenation of ethyl butyrate (EB)

While the hydrogenation of ethyl butyrate is expected to give 1-butanol and ethyl alcohol, measurable amounts of butyl butyrate, C_1–C_4 paraffins, and ethoxy butane were also observed in the products (Scheme 1). Conversion and selectivity data for hydrogenation of ethyl butyrate are provided in Table 1.

The percentage conversion of ethyl butyrate was high (~45%) during the initial period of time and reached a steady value after about 24 h of time on-stream. The selectivity to ethanol was 42.0–44.0%, while the selectivity to 1-butanol was 30.0–32.0%. In addition to alcohols, different side reactions (e.g., transesterification, dehydration, cracking) produced a measurable amount of butyl butyrate, ethoxy butane, and linear C_1–C_4 alkanes as by-products.

Deuterium switching was carried out after reaching a desirable conversion of ester in order to determine the nature of the isotope effect that exists for hydrogenation of ethyl butyrate. Ethyl butyrate conversion increased by a factor of ~1.81 (i.e., $k_H/k_D = 0.55$) and then returned to the baseline conversion level after switching back to hydrogen. The data in Table 2 and Fig. 1 demonstrate that hydrogenation of ethyl butyrate displays an inverse isotope effect and this deuterium isotope effect also exists for the rate of formation of 1-butanol and ethanol as well. The appearance of an inverse isotope effect for hydrogenation of ethyl butyrate to alcohol indicates that a hydrogen addition step is involved in the rate-determining step. In several studies of the hydrogenolysis of methyl and ethyl acetates, the authors advocate that hydrogenation proceeds via dissociatively adsorbed acetates [18]. Many suggest that hydrogenation of the acyl fragment is the rate-determining step during acetate hydrogenolysis over Cu/SiO_2 catalysts [9,11].

In the case of 25% Co/γ-Al_2O_3, the first question is whether the ethyl butyrate is adsorbed associatively or dissociatively. It is also important to shed light on the roles played by both the metal (Co) and support (γ-Al_2O_3) in adsorbing and turning over reactants and intermediates on the catalyst surface. Thus, ethyl butyrate adsorption was investigated on both the unpromoted support and cobalt catalyst by DRIFTS. These findings were then compared to the catalytic testing results to gain insight into the likely rate-determining step.

DRIFTS spectra for ethyl butyrate adsorption over γ-Al_2O_3 and 25% Co/γ-Al_2O_3 at various conditions are displayed in Fig. 2. Table 3 summarizes the vibrational bands and mode assignments for surface species formed from adsorption of ethyl butyrate followed by the introduction of H_2 at 493 K over γ-Al_2O_3 and 25% Co/γ-Al_2O_3. At 473 K under He, γ-Al_2O_3 exhibits bands in the 2760–3000 cm^{-1} region corresponding to CH_3 and CH_2 vibrational modes [e.g., ν (CH)] from adsorbed ethoxy and butanoate species. Characteristic ν (C–O) bands corresponding to mono- (ν

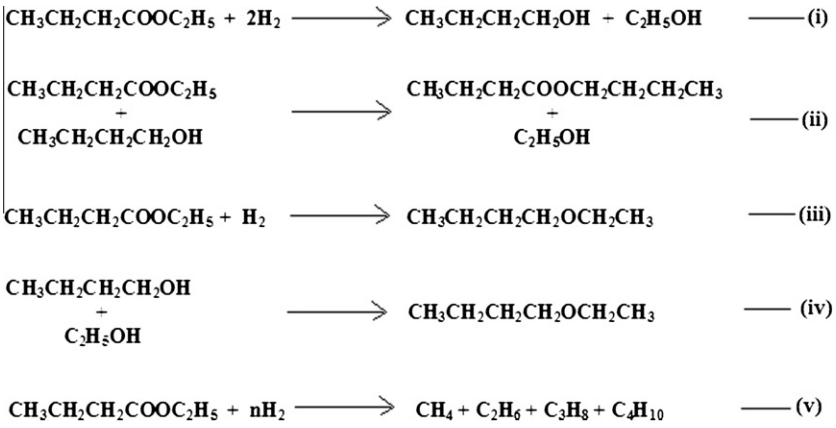

Scheme 1. Reaction scheme for the hydrogenolysis of ethyl butyrate over 25% Co/γ-Al_2O_3.

Table 1
Hydrogenation of ethyl butyrate over 25% Co/γ-Al_2O_3. (Temperature, 493 K; pressure 1.55 MPa; W/F (10^{-3}) = 24.6 g cat min L^{-1}.)

Time (h)	H_2/EB[b] ratio	% EB conversion	Selectivity (%)				
			Ethanol	1-Butanol	Ethoxy butane	Butyl butyrate	C_1–C_4[a]
20	4.0	24.0	43.6	30.7	6.9	12.7	6.1
26	4.0	24.5	43.5	31.4	6.8	12.7	5.6
43	4.0	17.8	44.1	30.8	6.6	12.3	6.2
51 (D_2)[c]	4.0 (D_2)	35.6 (D_2)	42.1	31.9	8.7	10.1	7.2
55 (D_2)	4.0 (D_2)	34.6 (D_2)	42.1	31.9	8.6	10.3	7.1
67.5	4.0	19.3	42.3	30.3	6.1	15.9	5.4
73.6	4.0	15.6	43.4	32.1	6.3	13.5	4.7

[a] Linear alkanes.
[b] EB represents ethyl butyrate.
[c] D_2 in the parenthesis indicate samples obtained from the deuterium switch.

Table 2
Deuterium isotope effect for hydrogenation of ethyl butyrate, butyric acid, and butyraldehyde over 25% Co/γ-Al_2O_3.

Compound (X)	H_2/(X) ratio	KIE on conversion (H/D)	Rates (r^H/r^D)				
			Ethanol	1-Butanol	Ethoxy butane	Butyl butyrate	C_1–C_4
Ethyl butyrate	4.0	0.50	0.64	0.61	0.46	0.99	0.57
n-Butyric acid	5.0	0.54	–	0.57	–	0.84	–
n-Butyraldehyde	4.0	0.98	–	0.95	–	–	–

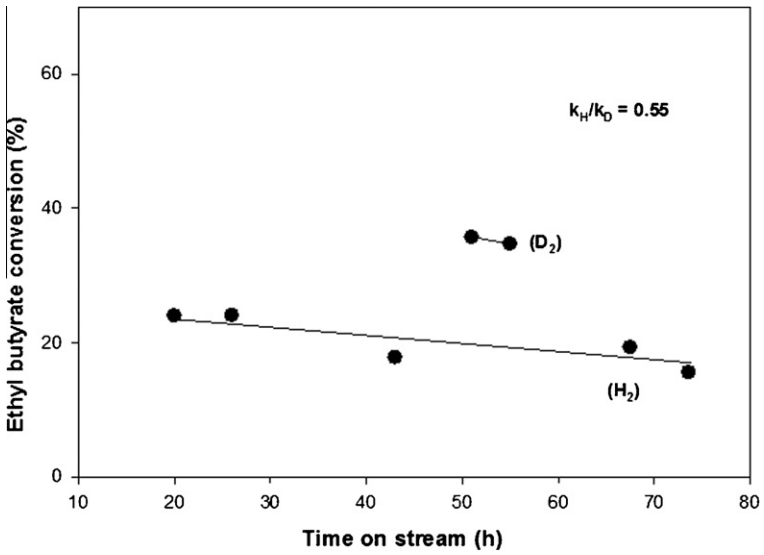

Fig. 1. Deuterium isotope effect observed during the conversion of ethyl butyrate over 25% Co/γ-Al_2O_3.

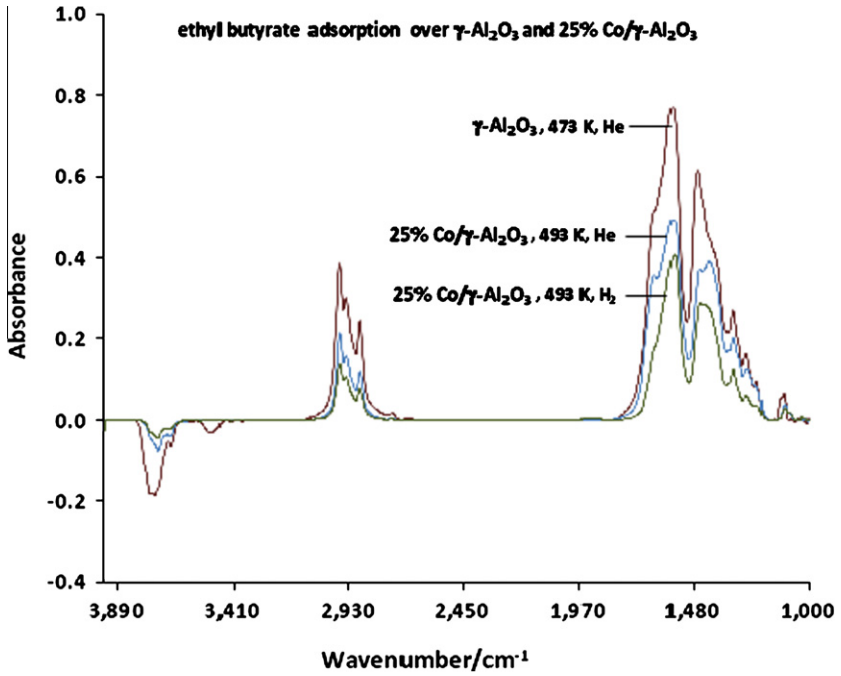

Fig. 2. DRIFTS spectra corresponding to ethyl butyrate adsorption over (a) γ-Al_2O_3 at 473 K under flowing He, (b) 25% Co/γ-Al_2O_3 at 473 K under flowing He, and (c) 25% Co/γ-Al_2O_3 at 493 K under flowing H_2.

Table 3
Infrared vibrational frequencies and mode assignments for surface species formed from the adsorption of ethyl butyrate followed by exposure to flowing H_2 at 493 K over γ-Al_2O_3 and 25% Co/γ-Al_2O_3.

Mode	γ-Al_2O_3	25% Co/γ-Al_2O_3
ν_{as} (CH_3)	2968	2967
ν_{as} (CH_2)	2940	2940
ν_s (CH_3)	2881	2881
ν_{as} (RCO)	1650	1644
ν_{as} (OCO)	1573	1564
	1613 (sh)	1605 (sh)
		1575 (sh)
ν_s (OCO)	1469	1459
	1446 (sh)	1439 (sh)
δ_{as} (CH_3)	1412	1420
	1386 (sh)	1385 (sh)
δ_s (CH_3)	1342	1338
	1317 (sh)	1315 (sh)
	1297 (sh)	1294 (sh)
τ (CH_2)	1264	1262
	1246 (sh)	1245 (sh)
ν (CO)	1191	1101
		1078

(CO) = 1100 cm^{-1}) and bi-dentate (ν (CO) = 1050 cm^{-1}) ethoxy species were observed for γ-Al_2O_3 and 25% Co/γ-Al_2O_3 samples at 473 K under helium indicating that ethyl butyrate adsorbs dissociatively to form ethoxy and butanoate species on γ-Al_2O_3. The presence of two dominant bands centered at 1573 and 1469 cm^{-1} correspond to asymmetric ν_{asymm} (–COO) and symmetric ν_{symm} (–COO) stretching of adsorbed butanoate species (i.e., CH_3–CH_2–CH_2–COO–, Scheme 2a) respectively, while a shoulder at 1650 cm^{-1} was ascribed to a butanoyl species (i.e., CH_3–CH_2–CH_2–CO–, Scheme 2b) resulting from the dissociative adsorption of ethyl butyrate on γ-Al_2O_3. A similar band at 1644 cm^{-1} was also observed for 25% Co/γ-Al_2O_3. An acetyl species characterized by an IR band at 1660 cm^{-1} has been reported on Co/ZnO after ethanol steam reforming at 673 K [19]. The absorbances of all these bands decrease under H_2 treatment at 493 K, suggesting that the dissociatively adsorbed butanoyl and butanoate species react with adsorbed hydrogen to form the respective alcohols.

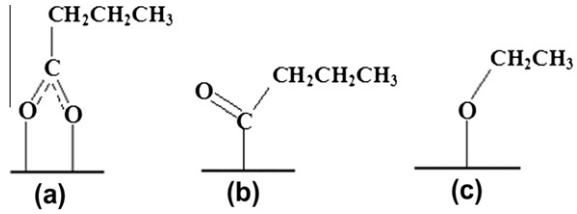

Scheme 2. Possible surface species formed from the adsorption of ethyl butyrate over 25% Co/γ-Al_2O_3 under flowing heat 473 K: (a) butanoate, (b) butanoyl, and (c) ethoxy species.

Characteristic bands (Fig. 2) corresponding to butanoate and butanoyl species are evident upon adsorption of ethyl butyrate under flowing He at 473 K over γ-Al_2O_3 and reveal that dissociative adsorption of ethyl butyrate takes place on the γ-Al_2O_3 surface. Furthermore, as shown in Scheme 2, there may be two kinds of dissociative adsorption: (1) cleavage of C–O within the ethoxy group of the ester (i.e., RCOO–R) to form a butanoate species (Scheme 2a) and ethane or (2) cleavage of the C–O (i.e., single bond, not the carbonyl) of the ester (RCO–OR) to form a butanoyl species (Scheme 2b). Similar species, like acetate and the acetyl species are well-known pseudo-stable intermediates for hydrogenolysis of ethyl and methyl acetates [20,21]. In addition to γ-Al_2O_3, ethyl butyrate could also adsorb dissociatively on metallic sites of cobalt.

Defect sites on γ-Al_2O_3 may be created during dehydration according to Peri's model [22], and these vacancy defects adjoin pair or triplet oxide defects providing unusual exposure of the aluminum ions in the underlying layer. Depending on the number of defect sites exposed at the surface of γ-Al_2O_3, one would expect that, in the case of RCO–OR' bond breaking, ethyl butyrate could dissociate in two possible ways to form butanoate and/or butanoyl surface intermediates (Scheme 3a and 3b). On the other hand, in the case of breaking of the RCOO–R' bond, butanoate species may form according to Scheme 3c. There are few examples available

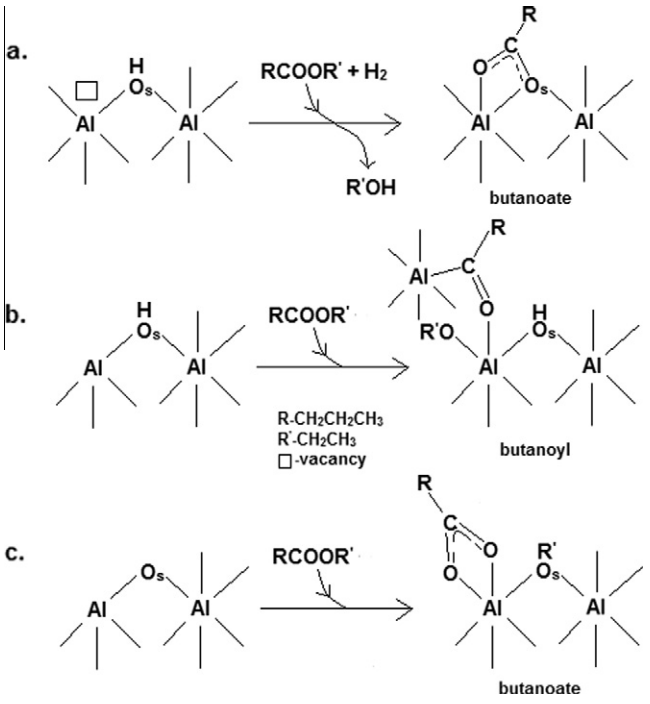

Scheme 3. The formation of butanoate and butanoyl species on γ-Al_2O_3.

in the literature regarding the stabilization of acyl species on γ-Al_2O_3 [16,23]. Bayman et al. [15] suggested from inelastic electron tunneling measurements on γ-Al_2O_3 that esters (RCOOR′) can dissociatively adsorb on γ-Al_2O_3. The authors further reveal that organic esters in general react with surface bound hydroxyl groups at acidic sites on the alumina surface to form symmetrical chemisorbed carboxylate anion species. Okumura et al. [24] demonstrated that, due to the lack of surface acidity on GeO_2/SiO_2, ethyl acetate dissociatively adsorbs as unidentate acetate and ethoxy groups during ethyl acetate hydrogenation on Rh/monolayer GeO_2/SiO_2 reduced at 423–523 K. Therefore, we believe that for the experimental conditions used, butanoate and butanoyl are pseudo-stable intermediates formed during ethyl butyrate hydrogenolysis covering the surfaces of both γ-Al_2O_3 and metallic cobalt.

Fig. 3 shows the TPD of adsorbed ethyl butyrate over 25% Co/γ-Al_2O_3 under flowing H_2. As temperature increases, the intensities of all the adsorption bands decrease, particularly the one at 1644 cm^{-1} associated with the butanoyl species. Compared to butanoyl species, butanoate appears to be more stable under our experimental conditions. Thus, hydrogenation of butanoate to partially hydrogenated intermediates could possibly be the rate-determining step in the hydrogenation of ethyl butyrate over 25% Co/γ-Al_2O_3. It is of interest to compare these results with the deuterium isotope effect for the hydrogenation of butyric acid, not only in that it may generate similar kinds of intermediates as from ethyl butyrate, but also from the point of view of hydrogenation activity.

3.2. Hydrogenation of n-butyric acid (BA)

The typical reaction conditions for hydrogenation of *n*-butyric acid are shown in Table 4. Unlike ethyl butyrate, which yielded a number of additional compounds, butyric acid hydrogenation selectively produces *n*-butanol (80–91%) in addition to forming butyl butyrate (8–10%). The data show that the catalyst deactivation rate was higher for butyric acid hydrogenation relative to ethyl butyrate hydrogenation, which may be attributed to the poisoning effect of butyric acid on cobalt sites. The deuterium isotope effect was obtained by comparing the hydrogenation activity of butyric acid with periods of addition of H_2 – then D_2 – and then switching back to H_2. The resultant deuterium isotope effect was measured directly by comparing the hydrogenation activity of butyric acid (r^H/r^D) and is displayed in Table 2 and Fig. 4. Hydrogenation of *n*-butyric acid follows an inverse isotope effect ($H/D = 0.54$), and the magnitude is similar to that of ethyl butyrate. Therefore, it is likely that similar intermediates are involved in the rate-determining step in the hydrogenation of both ethyl butyrate and *n*-butyric acid.

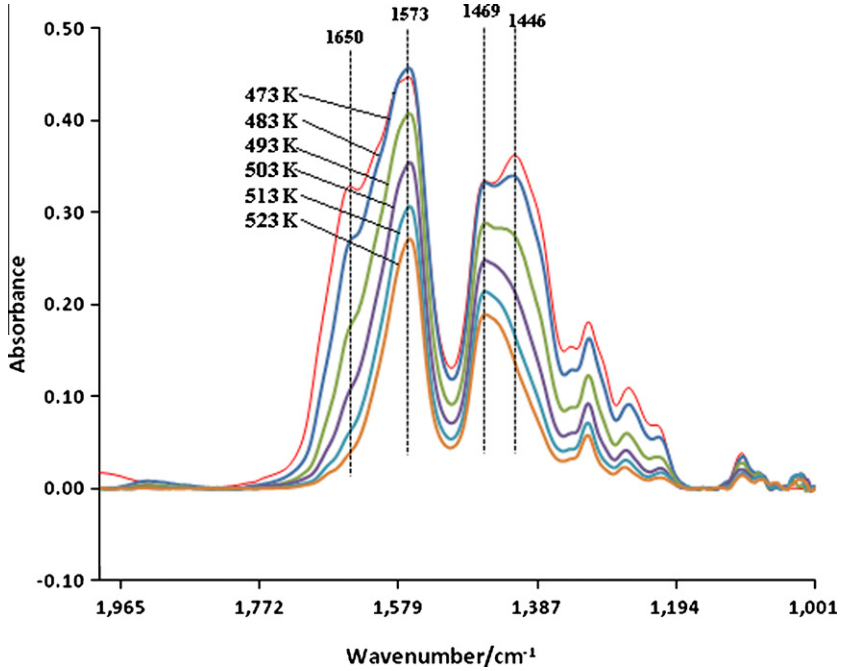

Fig. 3. DRIFTS-TPD spectra corresponding to ethyl butyrate adsorption over 25% Co/γ-Al_2O_3 under flowing H_2 (473–523 K).

Table 4
Hydrogenation of *n*-butyric acid over 25% Co/γ-Al_2O_3 (Temperature, 493 K; pressure 0.80 MPa; W/F (10^{-3}) = 5.69 g cat min L^{-1}).

Time (h)	H_2/*n*-butyric acid ratio	% *n*-Butyric acid conversion	Selectivity (%)		
			Acetone	*n*-Butanol	Butyl butyrate
1.00	5.0	62.9	10.2	81.6	8.2
4.00	5.0	39.8	3.5	86.8	9.7
6.30	5.0	11.2	2.6	87.5	9.9
9.95 (D_2)[a]	5.0 (D_2)	15.9 (D_2)	1.8	91.1	7.1
11.65	5.0	7.2	4.9	86.6	8.5
15.00	5.0	4.7	4.9	86.6	8.5

[a] D_2 in the parentheses indicate samples obtained from the switch to deuterium.

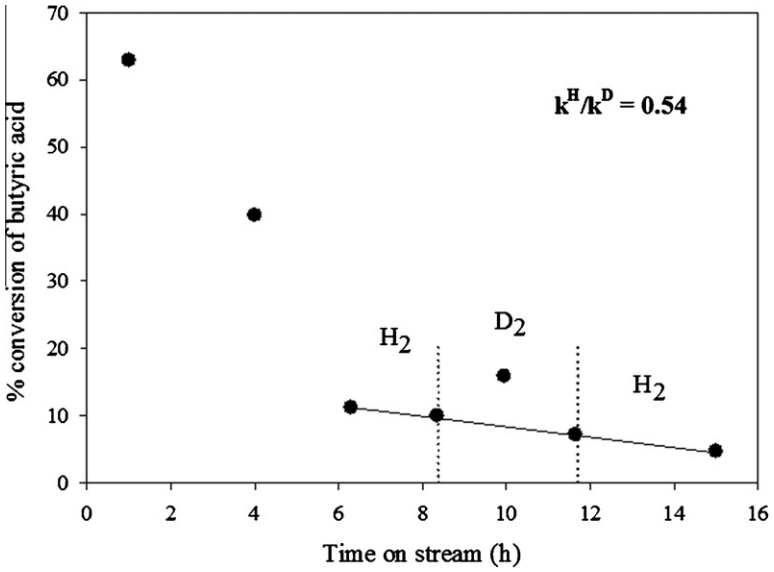

Fig. 4. Deuterium isotope effect observed during the conversion of *n*-butyric acid over 25% Co/γ-Al_2O_3.

DRIFTS experiments were carried out to follow the surface species formed upon adsorption of *n*-butyric acid on 25% Co/γ-Al_2O_3 at 473 K under He and H_2. The catalyst was reduced first in H_2 at 623 K and then the *n*-butyric acid was introduced using a syringe. Scans were taken in the range between 1000 and 4000 cm^{-1}. DRIFTS spectra obtained during *n*-butyric acid adsorption on 25%

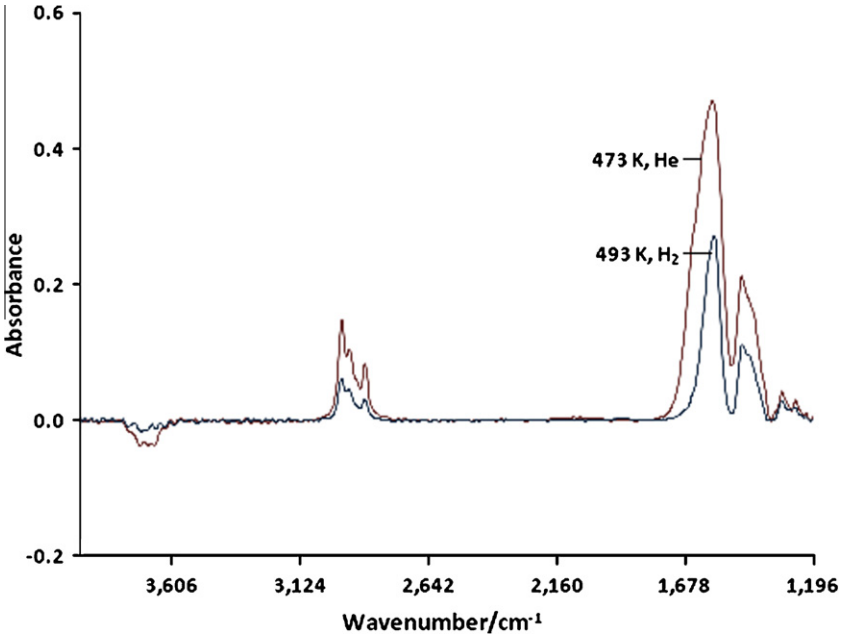

Fig. 5. DRIFTS spectra corresponding to *n*-butyric acid adsorption over 25% Co/γ-Al_2O_3.

Table 5
Infrared vibrational frequencies and mode assignments for surface species formed from the adsorption of *n*-butyric acid followed by exposure to flowing H_2 at 493 K over 25% Co/γ-Al_2O_3.

Mode	25% Co/γ-Al_2O_3
ν_{as} (CH_3)	2968
ν_{as} (CH_2)	2939, 2909 (sh)
ν_s (CH_3)	2881, 2830 (sh)
ν_s (CH_2)	2802
ν (CO)	1923
ν_{as} (OCO)	1575
	1600 (sh)
	1640 (sh)
ν_s (OCO)	1463
	1439 (sh)
	1422 (sh)
δ_s (CH_3)	1314
τ (CH_2)	1261
	1252

Co/γ-Al_2O_3 at different conditions are shown in Fig. 5. The DRIFTS spectra corresponding to 473 K under He display bands at 1575 and 1463 cm^{-1}, which are characteristic of asymmetric and symmetric vibrations of the O–C–O group in *n*-butyric acid. Similar band assignments of butanoate stretching vibrations, directly formed upon adsorption of *n*-butyric acid, have been reported for oxidized aluminum [25]. Table 5 shows the infrared bands observed for *n*-butyric acid adsorption on 25% Co/γ-Al_2O_3 after introducing flowing H_2 at 493 K. Several bands in the 2746–3000 cm^{-1} region were observed, and the bands at 2968, 2939, 2909, 2881, 2830 cm^{-1} may be attributed to ν (CH) stretching modes of CH_3– and CH_2– from the butyl group adsorbed on γ-Al_2O_3. Heating the 25% Co/γ-Al_2O_3 catalyst to 493 K under H_2 decreased considerably the band intensities of characteristic asymmetric and symmetric vibrations of butanoate species. This suggests that the dissociatively adsorbed H on cobalt could hydrogenate the adsorbed RCO_2- group on the oxide surface of γ-Al_2O_3 to form butanol. Using nonlocal density functional theory calculations, Pallassana and Neurock [26] concluded that C–O bond activation is likely to be the rate determining for hydrogenolysis of acetic acid on Pd-based catalysts. Natal-Santiago et al. [27,28] using microcalorimetry, infrared spectroscopy, and reaction testing for kinetics combined with quantum chemical calculations, demonstrated that the rates of reduction of acetic acid and alkyl acetates on Cu/SiO_2 catalysts appear to be determined by the dissociative adsorption of these molecules and the hydrogenation of surface acyl species. Our DRIFTS results for the hydrogenolysis of ethyl butyrate and *n*-butyric acid over Co/γ-Al_2O_3 suggest that butanoate is the dominant and more stable surface species under these experimental conditions.

Table 6 shows the distribution of d-isotopic isomer of butanol and ethanol formed while deuterium was used as the source for the hydrogenation of ethyl butyrate, *n*-butyric acid, and *n*-butyraldehyde. Deuterium addition to ethyl butyrate without any H/D exchange could generate three and one deuterium atoms per

Table 6
H/*D* exchange in the formation of alcohol.

Sample	D-distribution (mol%)									*d*/Molecule
	d_0	d_1	d_2	d_3	d_4	d_5	d_6	d_7	d_8	
Hydrogenation of ethyl butyrate										
1-Butanol	0	0	0	36.1	36	18.4	6.6	2.9	0	4.04
Ethanol	0	53.2	24	14.7	8.1	0	0	0	0	1.78
Hydrogenation of *n*-butyric acid										
1-Butanol	0	0	0	40	33.75	17.7	8.5	0	0	3.94
Hydrogenation of *n*-butyraldehyde										
1-Butanol	0	0	50.5	28.6	15.3	5.6	0	0	0	2.76

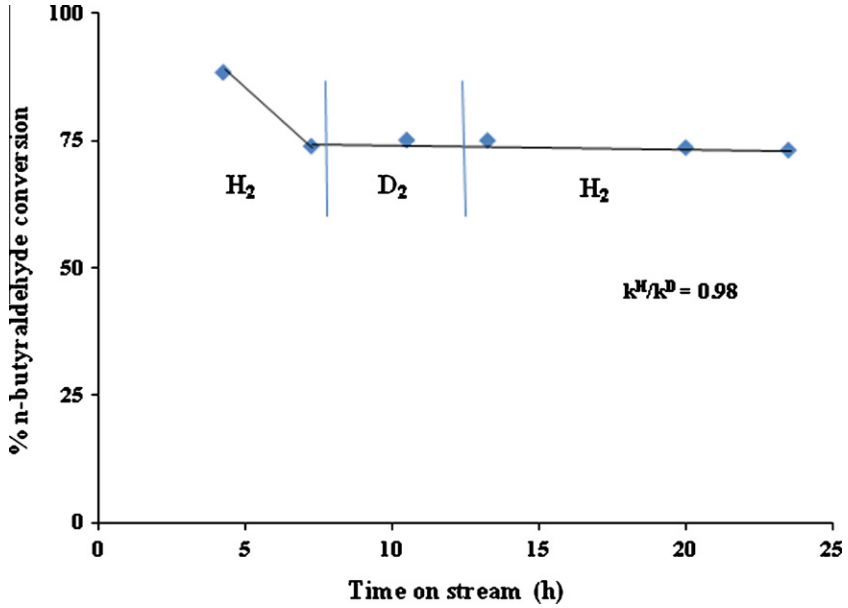

Fig. 6. Deuterium isotope effect observed during the conversion of *n*-butyraldehyde over 25% Co/γ-Al_2O_3.

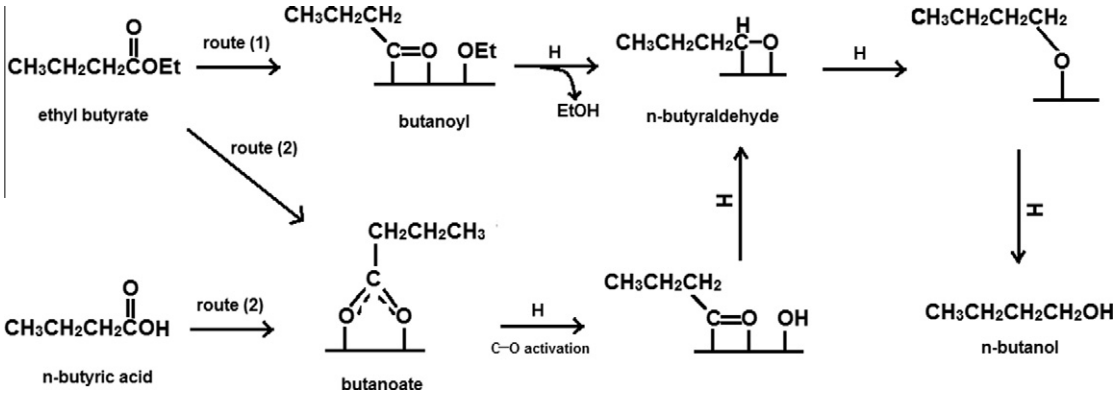

Scheme 4. A simplified reaction network for hydrogenation of ethyl butyrate and butyric acid over 25% Co/γ-Al_2O_3 at 493 K.

molecule of butanol and ethanol, respectively (Eq. (1)). However, we observed 4.04 and 1.78 deuterium atoms per molecule of butanol and ethanol, respectively. Similarly, for hydrogenolysis of *n*-butyric acid (Eq. (2)) and butyraldehyde (Eq. (3)) the observed number of deuterium atoms incorporated per molecule of butanol formed was slightly higher than the theoretical value. This indicates that *H*/*D* exchange occurs at the CH_2 position of alcohol intermediates while interacting on the surface of the catalyst, which leads to an excess in the number of deuterium atoms incorporated per molecule of alcohol formed.

$$CH_3CH_2CH_2COOC_2H_5 + 2D_2 \rightarrow CH_3CH_2CH_2CD_2OD + C_2H_5OD \quad (1)$$

$$CH_3CH_2CH_2COOH + 2D_2 \rightarrow CH_3CH_2CH_2CD_2OD + HDO \quad (2)$$

$$CH_3CH_2CH_2CHO + 2D_2 \rightarrow CH_3CH_2CH_2CHDOD + D_2O \quad (3)$$

In the conversion of either ethyl butyrate or *n*-butyric acid, deuterium analysis suggests that the residence times of intermediates are similar. Agarwal et al. [14], using IR spectroscopy, identified the acetyl intermediate during *in situ* hydrogenation of ethyl acetate over Cu/SiO_2, suggesting that acetyl species have significant surface lifetimes and are not rapidly hydrogenated to the acetaldehyde or alcohol. Although the catalyst system employed in that investigation was metallic copper, the adsorption of similar intermediates may be valid for Co/γ-Al_2O_3 as well, in which we presume that there is an availability of reaction intermediates adsorbed on the surface of γ-Al_2O_3, (i.e., surface fugacity) and that these intermediates further react at the Co/γ-Al_2O_3 interface. Thus, the butanoate (Scheme 2a) and butanoyl (Scheme 2b) hydrogenation steps to butyraldehyde, along with the further hydrogenation step to butanol, are the possible steps that may be kinetically significant.

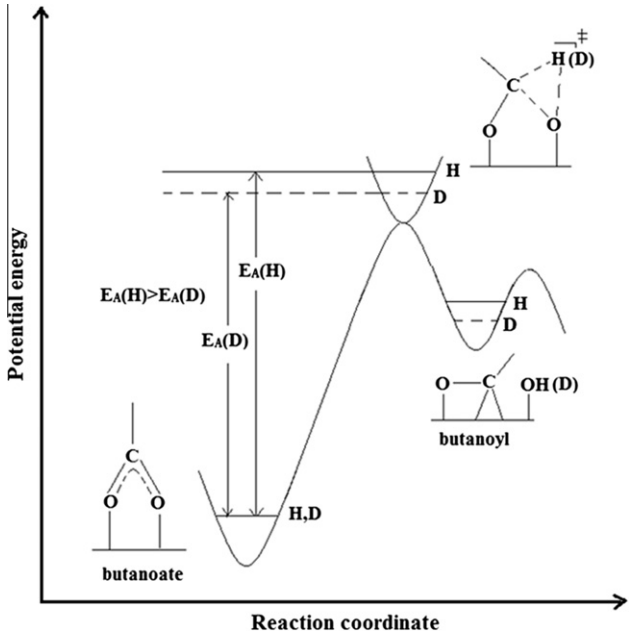

Scheme 5. Potential-energy profile.

In order to further distinguish the likely rate-limiting step, we have performed a deuterium switching experiment for hydrogenation of *n*-butyraldehyde to butanol and the corresponding data are displayed in Table 2 and Fig. 6. The hydrogenation of butyraldehyde to butanol does not display a deuterium isotope effect, indicating that hydrogen addition to adsorbed aldehyde is not likely involved in the rate-limiting step. Rachmady and Vannice [29] determined that the turnover frequency (TOF) for acetaldehyde hydrogenation on Pt/TiO_2 catalysts is 1000-fold higher than that of acetic acid hydrogenolysis. Agarwal et al. [14] demonstrated that the TOF for the conversion of acetaldehyde to ethanol is roughly 6000 times higher than that of ester hydrogenolysis under otherwise identical reaction conditions. In summary, we speculate that the formation of a partially hydrogenated intermediate species from butanoate and butanoyl is likely to be rate-controlling in the hydrogenolysis of ethyl butyrate and *n*-butyric acid on Co/γ-Al_2O_3 rather than either dissociation of ethyl butyrate/butyric acid or butyraldehyde hydrogenation.

The observed inverse isotope effect may be explained in the following manner. From the previous discussion, the hydrogenation of ethyl butyrate and *n*-butyric acid follows a butanoate or a very similar kind of intermediate species (Scheme 4), and hydrogenation of this species is the likely rate-limiting step. The KIE is a dependence of the rate of a chemical reaction on the isotopic identity of an atom in a reactant. Isotopic substitution can modify the rate of reaction due to the changes in the vibrational frequencies of reacting molecules. Scheme 5 shows a proposed potential-energy diagram for the activated complex formed on addition of *H* or *D* to an adsorbed butanoate intermediate. Here, we consider that the ground state energy level corresponding to *H* and *D* species are similar and tend to separate when they approach the activated state.

According to Scheme 5, the transition state, which involves C–O activation through C–D(H)–O bridging formation, is closer in energy to, and thus resembles more closely the product of that elementary step (i.e., the pseudo-stable butanoyl) rather than the reactants. Since the C–D bond is at lower energy than that of C–H in the transition state, an inverse isotope effect should result if

that specific step is rate limiting. Note also the change in carbon hybridization from sp^2 to sp^3 along the reaction coordinate and this bonding change may lead to an IKIE. Similar effects are known in organic reactions [30]. Therefore, it is possible to conclude that hydrogenation of ethyl butyrate and butyric acid follows an inverse isotope effect where hydrogen addition to C–O is the rate-limiting step. At this stage, the possibility that the hydrogenation of butanoyl species rather than butanoate is involved in the rate-determining step cannot be completely ruled out.

4. Conclusions

$Co/\gamma\text{-}Al_2O_3$ catalysts are active for the conversion of ethyl butyrate to *n*-butanol at moderate temperatures and pressures. Hydrogenation of ethyl butyrate and *n*-butyric acid follows an inverse kinetic isotope effect. The DRIFTS study indicated that two kinds of dissociative adsorption of ethyl butyrate are possible on the catalyst surface under the conditions followed. Butanoate and butanoyl species are the pseudo-stable surface intermediates, and hydrogenation of one of these intermediates is likely involved in the rate-limiting step of ethyl butyrate and butyric acid hydrogenation for the $\gamma\text{-}Al_2O_3$-supported cobalt system.

References

[1] H. Adkins, Org. Reactions 8 (1984) 1.
[2] P.E. Peterson, C. Casey, J. Org. Chem. 29 (1964) 2325.
[3] M. Zdrazil, Collect. Czech. Chem. Commun. 39 (1974) 1488.
[4] A.P.G. Kieboom, J.F. de Kreuk, A. van Bekkum, J. Catal. 20 (1971) 58.
[5] J.D. Chanley, T. Mezzetti, J. Org. Chem. 29 (1964) 228.
[6] K. Turner, M.W. Tuck, 12th NAM of the Catalysis Society, Lexington, KY, 1991.
[7] B. Miya, US Patent 3894,054 (1975) to Kao Soap Company, Ltd., Japan.
[8] M. Kitson, P.S. Williams, US Patent 4985,572 (1991) to The British Petroleum Company, London.
[9] T.Y. Yan, L.F. Albright, L.C. Case, Ind. Eng. Chem. Prod. Res. Dev. 4 (1965) 101.
[10] J.W. Evans, N.W. Cant, D.L. Trimm, M.S. Wainwright, Appl. Catal. 6 (1983) 355.
[11] P. Claus, M. Lucas, B. Lucke, T. Berndt, P. Birke, Appl. Catal. A: Gen. 79 (1991) 1.
[12] F.Th. Van de Scheur, L.H. Staal, Appl. Catal. A: Gen. 108 (1994) 63.
[13] P.A. Sorum, O.T. Onsager, Proc. Int. Congr. Catal. 8 (1984) 233.
[14] A.K. Agarwal, N.W. Cant, M.S. Wainwright, D.L. Trimm, J. Mol. Catal. 43 (1987) 79.
[15] A. Bayman, P.K. Hansma, L.H. Gale, Surf. Sci. 125 (1983) 613.
[16] R. Kieffer, J.P. Hindermann, R. El Bacha, A. Kiennemann, A. Deluzarche, React. Kinet. Catal. Lett. 21 (1982) 17.
[17] A.D. Buckland, J. Graham, R. Rudham, C.H. Rochester, J. Chem. Soc. Faraday Trans. I 77 (1981) 2845.
[18] T. Turek, D.L. Trimm, N.W. Cant, Catal. Rev. Sci. Eng. 36 (1994) 645.
[19] J. Llorca, N. Homs, P. Ramirez Piscina, J. Catal. 227 (2004) 556.
[20] M.A. Kohler, N.W. Cant, M.S. Wainwright, D.L. Trimm, Proc. Int. Cong. Catal. 9 (1988) 1043.
[21] J.W. Evans, M.S. Wainwright, N.W. Cant, D.L. Trimm, J. Catal. 88 (1984) 203.
[22] J.B. Peri, J. Phys. Chem. 69 (1965) 220.
[23] A.V. Deo, T.T. Chang, I.G. Dalla Lana, J. Phys. Chem. 75 (1971) 234.
[24] K. Okumura, K. Asakura, Y. Iwasawa, J. Phys. Chem. B 101 (1997) 9984.
[25] F.J. Jouwslager, A.H.M. Sondag, Langmuir 10 (1994) 1028.
[26] V. Pallassana, M. Neurock, J. Catal. 209 (2002) 289.
[27] M.A. Natal-Santiago, M.A. Sanchez-Castillo, R.D. Cortright, J.A. Dumesic, J. Catal. 193 (2000) 16.
[28] M.A. Natal-Santiago, M. Hill Josephine, J.A. Dumesic, J. Mol. Catal. A: Chem. 140 (1999) 199.
[29] W. Rachmady, M.A. Vannice, J. Catal. 192 (2000) 322.
[30] K.B. Wiberg, Chem. Rev. 55 (1955) 713.